Integration of genetically modified *virus-like-particles* with an optical resonator for selective bio-detection

2015 Nanotechnology 26 205501

(http://iopscience.iop.org/0957-4484/26/20/205501)

IOP Publishing Nanotechnology
Nanotechnology **26** (2015) 205501 (9pp) doi:10.1088/0957-4484/26/20/205501

Integration of genetically modified *virus-like-particles* with an optical resonator for selective bio-detection

X Z Fan[1], L Naves[2], N P Siwak[1], A Brown[3], J Culver[2,4] and R Ghodssi[1,3]

[1] MEMS Sensors and Actuators Laboratory, Departments of Electrical and Computer Engineering, Institute for Systems Research, University of Maryland, College Park, MD 20742, USA
[2] Institute for Bioscience and Biotechnology Research, University of Maryland, College Park, MD 20742, USA
[3] Fischell Department of Bioengineering, University of Maryland, College Park, MD 20742, USA
[4] Department of Plant Sciences and Landscape Architecture, University of Maryland, College Park, MD 20742, USA

E-mail: ghodssi@umd.edu

Received 10 December 2014, revised 2 March 2015
Accepted for publication 25 March 2015
Published 27 April 2015

Abstract

A novel *virus-like particle* (TMV-VLP) receptor layer has been integrated with an optical microdisk resonator transducer for biosensing applications. This bioreceptor layer is functionalized with selective peptides that encode unique recognition affinities. Integration of bioreceptors with sensor platforms is very challenging due their very different compatibility regimes. The TMV-VLP nanoreceptor exhibits integration robustness, including the ability for self-assembly along with traditional top-down microfabrication processes. An optical microdisk resonator has been functionalized for antibody binding with this receptor, demonstrating resonant wavelength shifts of ($\Delta\lambda_o$) of 0.79 nm and 5.95 nm after primary antibody binding and enzyme-linked immunosorbent assay (ELISA), respectively, illustrating label-free sensing of this bonding event. This demonstration of label-free sensing with genetically engineered TMV-VLP shows the flexibility and utility of this receptor coating when considering integration with other existing transducer platforms.

Keywords: optical ring resonator, bionanostructure, immunoassay

(Some figures may appear in colour only in the online journal)

Introduction

The detection and identification of biomolecules (e.g. antibodies, proteins, and peptides) is of increasing importance for a wide range of biological sciences and biomedical applications. The primary goals and challenges shared by all sensor systems are to achieve high sensitivity while at the same time maintaining selectivity. Furthermore, the efficiency and the speed of detection are criteria of increasing importance due to the cost of consumables associated with conventional schemes. There is a strong motivation and incentive to develop small, low-powered, easy-to-use microsystems to replace conventional macro-scale sensors for the identification of chemical or biological analytes. Miniaturized devices boast a small footprint, low power consumption, and easy read-out and integration schemes. They benefit from the high sensitivity and reliability of a wide range of microtransducer platforms and technologies. However, they often lack selectivity because of challenges associated with the practical integration of selective receptor layers due to their vastly different material properties and required fabrication and synthesis techniques.

Non-organic materials are typically used to fabricate microtransducers due to established fabrication techniques. The surface chemistry of these materials, typically without inherent selective recognition properties, is not easily tailored for recognition purposes. As a result, an additional receptor layer is needed to provide the desired recognition capabilities.

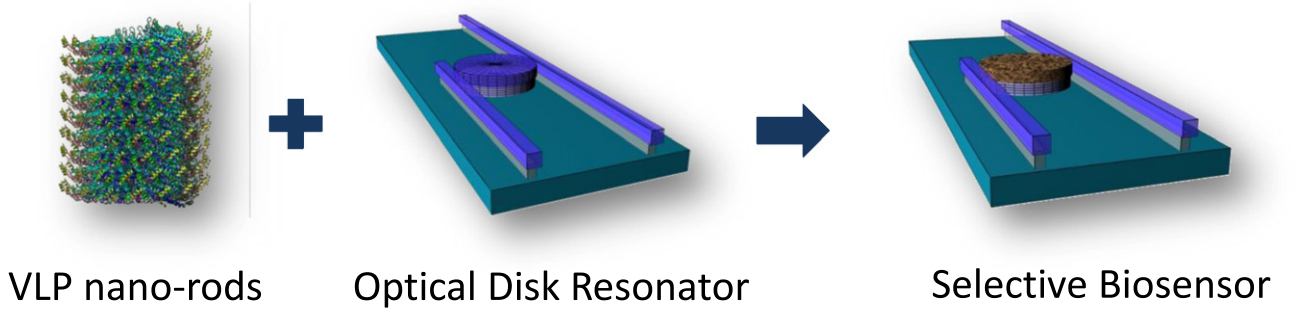

Figure 1. Schematic of the integration of TMV-VLP bioreceptor layer with an optical microdisk resonator to realize a biosensor system

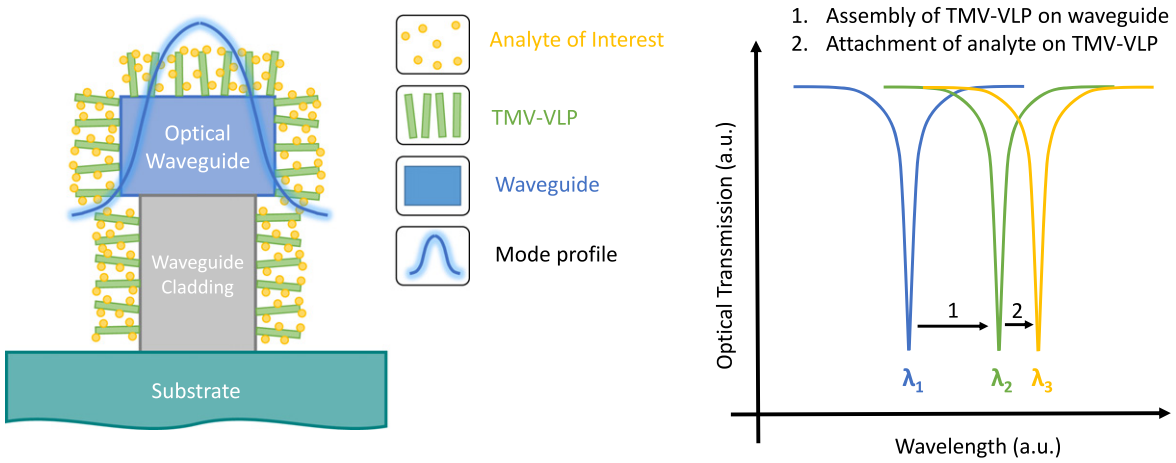

Figure 2. The diagram shows the principle of operation of the sensor system. The assembly of TMV-VLP will induce a shift in resonant wavelength due to the change in effective refractive index of the waveguide. The attachment of analyte to the TMV-VLP receptors will induce a further shift in resonant wavelength due to their interaction with the waveguide's evanescent field.

For biological sensing, biological systems already possess a plethora of key-lock pairs (complementary DNA strands [1], antibody-antigen [2], peptide-peptide [3], etc) that can be used to determine their receptor-analyte recognition properties. Advancements in protein engineering and phage display can further expand upon naturally occurring receptors by engineering bioreceptors that can potentially revolutionize sensor technologies through the adaptation of unique and targeted recognition affinities [4]. The potential of these bioreceptors is currently limited by integration challenges. Their robust integration with sensor platforms is very challenging because compatibility needs to be met at multiple levels, including processing integration and biofunctionality. Traditional top-down surface and bulk micromachining processes used to make microtransducers require high temperatures, extreme pH levels, and high vacuum, conditions that are not favorable for active biomolecules' survival. Conversely, biomolecules typically reside in conductive and corrosive aqueous solutions, which cause significant problems for high-Q mechanical resonators and electrical interrogation techniques. The challenge is to find a solution for robustly integrating these two very different domains in order to realize a highly sensitive and selective biosensing system.

The enabling technology in this work is a highly robust and genetically engineered bio-nanostructure called a *virus-like-particle* (TMV-VLP). TMV-VLPs are high-surface nanotubes of ~18 nm in diameter assembled from modified capsid coat proteins (CP) derived from *Tobacco mosaic virus* (TMV). The TMV-VLP macromolecule is structurally and functionally robust and demonstrated its bottom-up assembly compatibility with limited top-down patterning techniques [5–7]. Its 3D nanostructure maintains its structural integrity in both hydrated and dehydrated states. Furthermore, these biomolecule platforms feature a wide variety of genetically programmable functional groups [8, 9]. These include cysteines that facilitate self-assembly onto various substrates and sites for the display of receptor peptides with high affinity to target molecules.

The expression of these highly selective TMV-VLP bioreceptors on the active surface of sensitive refractive index (RI) optical microresonators results in an ideal versatile platform for on-chip biosensing (figure 1). The realization of this biosensor system is used to investigate and perform enzyme-linked immunosorbent assays (ELISA) for the detection of Flag antibody as a model system, using an established model antigen-antibody method. The sensitivity of this sensor platform has the potential to recognize this immunoassay in a label-free manner, simplifying traditional ELISA procedures.

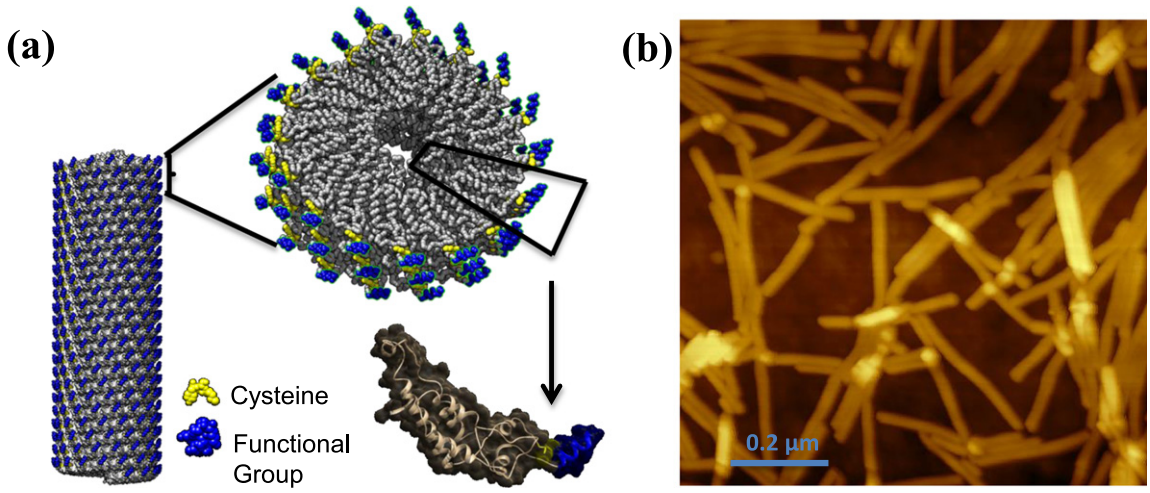

Figure 3. (a) Schematic showing the conjugation of TMV-VLP, expressing two possible functional groups. The TMV-VLP nanostructure consists of identical coat protein (CP) subunits assembled into a helical formation. Each CP can be conjugated with a multitude of motifs, including cysteines (shown in yellow) and antigen peptides (shown in blue) used in this work. (b) AFM images showing self-assembled TMV-VLP nanorods on a gold coated substrate.

Principle of operation

Optical transduction mechanism

Figure 2 shows a simplified overview of the sensor system's principle of operation. A functionalized TMV-VLP layer is assembled on an optical microdisk resonator to conduct antibody sensing via ELISA. The transduction mechanism of a microdisk resonator is based on changes in the cladding refractive index brought about by the attachment of analytes on the receptor layer that coats this optical resonant cavity [10]. These types of sensors provide high sensitivity and real-time measurement without labeling in both aqueous and dry conditions. A change in the surface condition of the resonator due to analyte binding onto this receptor layer will cause a change in the cladding's refractive index and thus a change in the effective RI (n_{eff}) of the sensor cavity as a whole. This optical change induces a measurable shift in the resonant wavelength ($\Delta\lambda_o$) of the cavity. Acquiring the optical spectrum of the resonator and tracking its $\Delta\lambda_o$ allows for surface binding events to be monitored in real time [11–13].

Selective binding mechanism

The selective bioreceptor layer, TMV-VLP (figure 3), takes advantage of its programmable surface to express high affinity binding probes and colored outer surface peptides. We have genetically engineered the TMV-VLP bioreceptor to express receptor peptides from the surface exposed carboxyl terminus of virus capsid coat proteins, magnified in figure 3(a), so as to act as a probe for a specific antibody. The yellow highlighted cysteine amino acid enables the self-assembly of TMV-VLP onto the substrate surface, and the blue highlighted functional groups provide the binding specificity towards the analyte of interest. Furthermore, the TMV coat proteins have been genetically modified to neutralize repulsive intersubunit carboxylate residues as a means to induce the self-assembly of the coat protein without the need for viral nucleic acid [14].

A traditional method for the detection and monitoring of antibodies or antigens is through ELISA, a widely used biochemical assay that utilizes a solid-phase enzyme immunoassay to monitor their presence in a liquid or wet environment. More specifically, the typical steps of a sandwich ELISA process include (1) immobilization of a capture antigen on a plate surface, (2) addition of a primary antibody to selectively bond to the immobilized antigen, (3) introduction of a secondary antibody, with a color-changing enzyme, to specifically bind to the primary antibody, and finally (4) exposing the sandwich chain to a substrate indicator which causes the enzyme to produce a colored substrate that can be visualized via optical inspection. Due to the high assay sensitivity, easy colorimetric read-out method, and broad applications, ELISA's miniaturization into an on-chip platform (ELISA-on-a-chip) has been widely studied [15–17]. The sensitivity of this hybrid bioreceptor optical transducer platform is used to perform traditional ELISA as well as label-free ELISA to simplify and reduce the number of steps required for antibody detection.

Design and methods

Optical transducer platform

Optical whispering-gallery mode resonators are designed to optimize their sensitivity through the maximization of the wave-to-analyte interaction. The wave interaction with the analyte is restricted within the evanescent field located on the surface of the resonator, whose intensity decays exponentially with increasing distance normal to the surface of the disk. Optimization of the sensor design is carried out by simulating the optical mode profiles and obtaining the electric field intensity of the evanescent field via the COMSOL

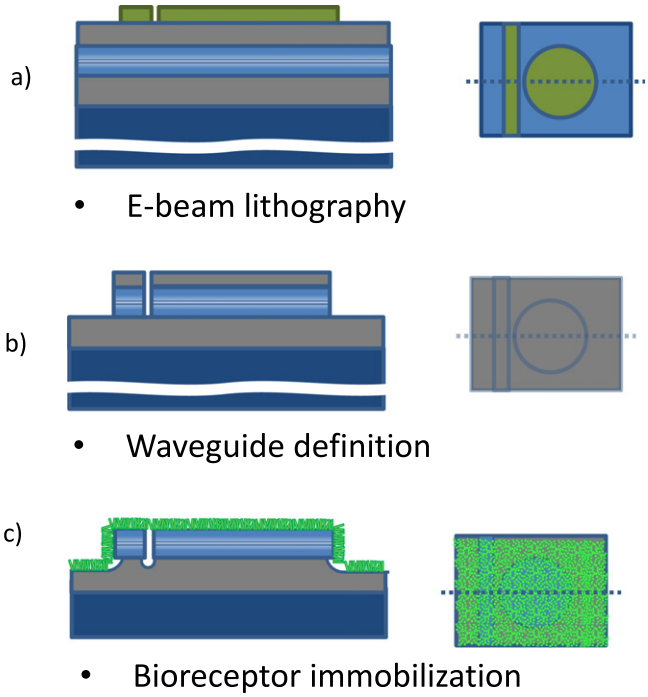

Figure 4. An abridged schematic of the microdisk resonator fabrication process flow showing (a) E-beam lithography patterning at the die level, (b) waveguide pattern transfer into the Si_3N_4 waveguide layer, and (c) immobilization of TMV-VLP bioreceptors onto the surface of the fabricated microdisk resonator.

Multiphysics package for varying dimensions. The simulation results and fabrication process limitations are used to directly inform the minimum and maximum waveguide dimensions and coupling gaps.

The 20 μm diameter and 340 nm thick silicon nitride on silicon dioxide microdisks are fabricated based on the abridged process flow shown in figure 4. The structure is patterned using E-beam lithography to define the optical waveguide and cavity on a 1.0 μm thick oxide mask. Reactive ion etching (RIE) with fluorine-based chemistry (CHF_3, O_2) is used to transfer the para-Methoxymethamphetamine (Micro-Chem PMMA) resist pattern into the oxide mask and subsequently into the silicon nitride waveguide layer. The process recipes are optimized to produce a vertical and smooth sidewall in order to decrease optical scattering losses. To minimize optical losses when light is coupled onto and off of the chip from external instrumentation via lensed fibers, the silicon substrate is thinned to ~150 μm to facilitate planar and more accurate cleaving of the input and output facets.

Bioreceptor layer

The TMV-VLP is a genetic derivation of the *Tobacco mosaic virus*. The *Tobacco mosaic virus* is composed of over 2130 identical coat proteins attached to a helical RNA backbone forming a nanorod. Each coat protein is a folded chain of amino acids with both end terminals (*c* and *n*) expressed on the outer surface. Each terminus can be genetically conjugated to express additional series of amino acids as binding probes. To realize TMV-VLP, the TMV coat proteins are further genetically engineered in order to self-replicate and self-assemble into nanorods in bacterial cells. This modified system allows the modification of the viral coat protein in the absence of virus replication and enables protein expression of TMV coat proteins and self-assembly of *virus-like-particles* directly in bacteria. As a result, this addresses problems associated with recombination and construct instability and dramatically decreases the synthesis period from 3 weeks to 48 h. The modification allows for TMV-VLP to replicate without the need for a helical RNA backbone due to the mutation of repulsive carboxylate residues E50Q and D77N. These mutations promote the self-assembly of capsid proteins into helical nanorods using a codon optimized for expression in *E. coli*. A more detailed description of the synthesis and purification process of the TMV-VLP can be found in [14].

The TMV-VLP constructs presented here include TMV1*cys*-and VLP-*Flag*. These VLP constructs include the addition of a cysteine residue at position 2 of the *n*-terminus. The addition of the cysteine thiol group (1*cys*) has been shown to promote the end-on attachment of the virus particles to numerous substrates including gold, silicon, polymers, and even dielectrics [5, 18, 19]. On the outer surface of the helical nanorod, they have been used as activation sites for noble metal nanoparticles produced by decomposition of Pt(II) or Pd(II) [1, 11]. In addition to the 1*cys* addition, TMV*1cys*-VLP-*Flag* expresses the antigen peptide (DYKDDDDK) from the *c*-terminus for the selective binding of Flag antibodies to create a high aspect ratio selective receptor. This position places the Flag peptide at the outer surface of each assembled capsid protein. Combined, these modifications yield a high surface area platform capable of oriented attachment onto defined surfaces as well as the display of multiple receptor peptides from each TMV-VLP rod.

Experimental procedure

The resonator's optical characteristics are evaluated using a tunable laser (Venturi Tunable Laser TLB-6600) with a tuning range of (1520 nm–1620 nm) synchronized with a high-speed photodetector (New Focus Model 1811). The laser signal is coupled onto and off of the chip using lensed single-mode fibers by coupling the light to the input port and capturing the light from the drop port, respectively. To obtain an optical spectrum of the resonator under test, the tunable laser output wavelength is triggered synchronously with the acquisition photodetector via LabVIEW, where the acquired signal is then correlated with wavelength. Spectral data can then be fitted to a Lorentzian curve to determine the quality (Q) factor and resonant wavelength of the system.

A baseline spectrum is collected from an uncoated transducer. This is followed by the self-assembly of two strands of TMV-VLPs (TMV1*Cys*-VLP-*Flag* and TMV1*Cys*-VLP), via their exposed cysteine, on the bottom of their nanorod on two different microdisk resonator chips. They were self-assembled by submerging the devices in a buffer solution with approximately 0.2 mg mL^{-1} concentration of

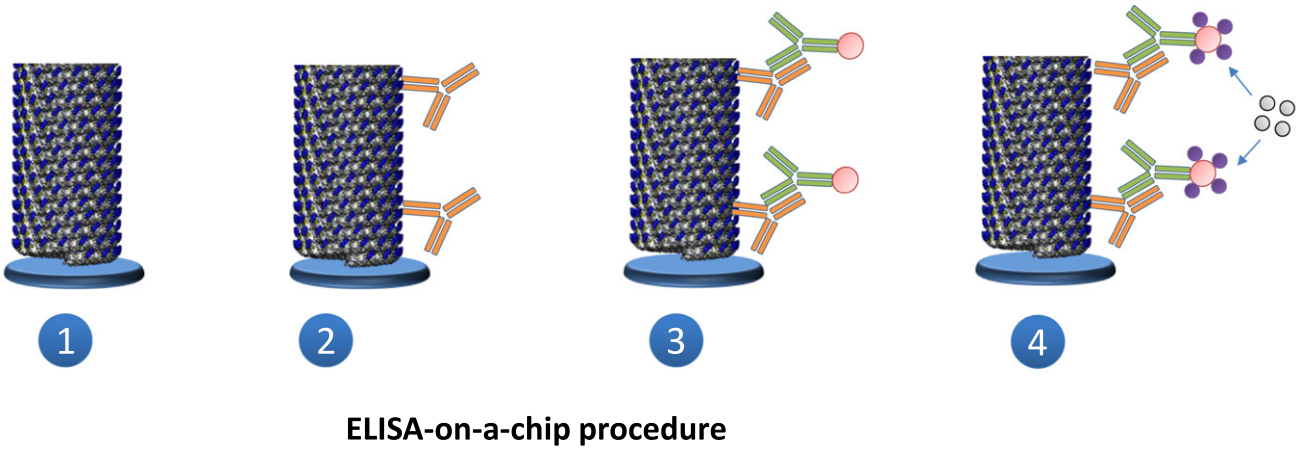

Figure 5. Process flow showing ELISA-on-a-chip procedure after the immobilization of TMV-VLP probes on a microdisk resonator.

TMV-VLPs for a 12 h period at room temperature. TMV1*Cys*-VLP-*Flag* receptor coating is used to selectively bind to Flag antibodies, and TMV1*Cys*-VLP (without the selective peptide) is used as a negative control to monitor any unspecific bindings to the surface of the transducer and the TMV-VLP bio-nanostructure. Both set of chips undergo identical ELISA procedures (abridged in the following steps and depicted in figure 5):

(1) The TMV1*Cys*-VLP decorated optical resonator is immersed in 5% non-fat milk in Tris buffered saline (TBS) (50 mM Tris-HCL, 200 mM NaCl, TBS) pH 7.0 for 30 min at room temperature as a blocking step to block any non-specific binding sites (blocking agents not explicitly shown in diagram).

(2) The chip is transferred to a 1/1000 dilution of primary antibody (depicted in orange) sera in TBS and 5% non-fat milk solution for 2 h at room temperature. The chip is then rinsed with TBS and TBS with 0.05% Tween 20 detergent (TBS-Tween).

(3) The chip is transferred to a 1/5000 dilution of secondary antibody (depicted in light green) sera, anti-rabbit alkaline phosphatase, in TBS 5% non-fat milk for an additional 2 h at room temperature. A similar TBS/TBS-Tween rinse as step (2) is carried out.

(4) Finally, enzyme substrate (color indicator) in substrate buffer is used to catalyze the enzyme, now decorated on each attached antibody, to a violet color.

The optical spectrum of the resonator is taken before and after TMV-VLP coating to investigate the Δn_{eff} due to receptor coating. The optical spectrum is compared before and after the ELISA procedure to investigate the response of the full ELISA procedure. The sensitivity of the platform allows for the optical monitoring of each stage of ELISA and exploration of the possibility of simplifying the process by eliminating the need for labeling with color indicator and/or secondary antibodies.

The selectivity of the bioreceptor layer is investigated against non-fat milk solution and non-complementary antibodies (anti-HA and anti-His). Non-fat milk is used because it contains a multitude of amino acids, proteins, vitamins, and minerals that could nonspecifically bind to the sensor surface. His-Tag and HA-Tag antibodies detect recombinant proteins containing the 6xHis and the HA epitope tag, respectively, neither of which is present in TMV1*Cys*-VLP-*Flag* or TMV1*Cys*-VLP structures.

All optical characterization of the resonator is conducted in a rinsed and dehydrated state in order to facilitate the measurement with the optical transducer. The effects of the rinse and dehydration procedure on the chip are independently investigated by conducting ELISA tests on gold-coated Si chips. The full protocol of ELISA is conducted on two sets of gold-coated chips. Each set is immobilized with four different concentrations of TMV1*Cys*-VLP-*Flag* receptors: 10^{-2} mg ml^{-1}, 10^{-4} mg ml^{-1}, 10^{-6} mg ml^{-1}, and 0 mg ml^{-1}. The first set of chips undergoes traditional ELISA, per the procedure listed, and is used as a control. The second set of chips undergoes a modified ELISA procedure where a rinsing and dehydration step is inserted between each biomolecule assembly step, resulting in a total of three dehydration and rehydration steps. Final color intensity changes between the two sets are compared by image analysis, in order to determine the level of preserved functionality of the dehydrated and rehydrated biomolecules.

Results

The minimum detectable wavelength shift of the sensor system is 16.89 pm, 3 times the standard deviation of the resonant wavelength ($\delta = 5.63$ pm) over a standard sensing experiment period of 72 h (from pre-TMV1*Cys*-VLP assembly until post ELISA procedures), which corresponds to a Δn_{eff} of 1.59×10^{-5} refractive index unit (RIU).

Figure 6 shows SEM images of a microdisk resonator before and after overnight bioreceptor assembly. The post-assembly image, figure 6(b), shows conformal nanostructure coverage on the optical waveguide and disk cavity. The nanostructures are coated with a thin film of metal in this SEM image to capture their 3D structure and increase imaging resolution. Nanostructures are shown to assemble even

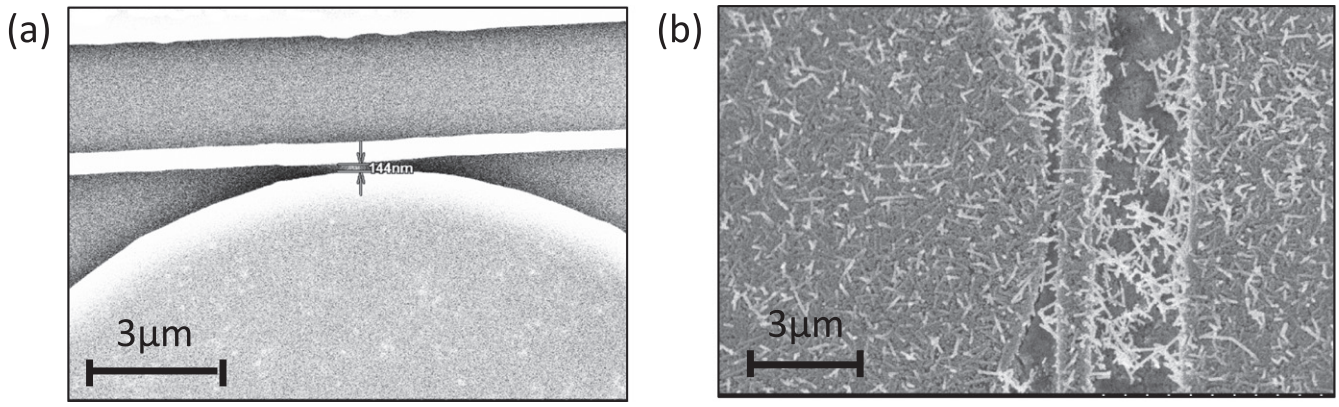

Figure 6. SEM images showing a microfabricated microdisk resonator (a) pre-TMV-VLP assembly and (b) post-TMV-VLP assembly.

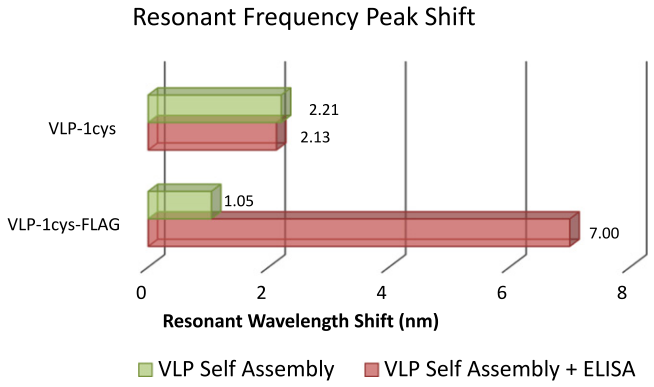

Figure 7. Resonant wavelength shift due to the assembly of TMV-VLPs, followed by conducting ELISA-on-a-chip

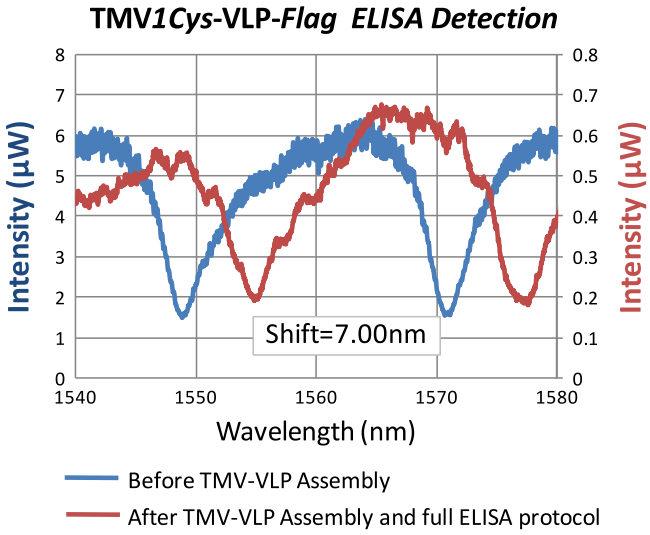

Figure 8. Optical frequency spectra showing the shift in resonant wavelength due to the assembly of TMV1*Cys*-VLP-*Flag* on a microdisk resonator, the attachment of primary and secondary antibodies, and the expression of enzymatic substrate (full ELISA protocol).

in the sub-micron (~114 nm) coupling gap. The optical spectrum taken before and after the 12 h TMV-VLP attachment shows resonant wavelength shifts of 2.21 +/− 0.34 nm and 1.05 +/− 0.23 nm for TMV*1Cys*-VLP and TMV*1Cys*-VLP-*Flag*, respectively. The 2.21 nm and 1.05 nm shifts correspond to effective refractive index shifts of 2.08×10^{-3} and 0.99×10^{-4} RIU, respectively. Based on SEM imaging, the morphology of the two types of TMV-VLPs shows a small variation in TMV-VLP coating density. TMV1*Cys*-VLP coating is denser and more uniformly conformal than TMV1*Cys*-VLP-*Flag*'s coverage. The variability in the wavelength shift within each type of TMV-VLP assembly is attributed to the randomness of the nanostructure assembly on the surface of the disk resonator and the variation between batches of TMV-VLP synthesis and purification. The TMV-VLP assembly, as observed in the SEM image in figure 6, shows non-uniform assembly across the surface. The length, orientation, and density of the TMV-VLP on the surface of the resonator will influence the propagating wave–receptor layer interaction and change the effective refractive index differently depending on these specifics.

Conducting the entire ELISA protocol on both TMV1*Cys*-VLP- and TMV1*Cys*-VLP-*Flag*-coated microdisk resonators results in resonant wavelength shifts of −0.08 +/−0.57 nm and 5.95 +/−2.68 nm, respectively, corresponding to a −3.62% and a +567% relative shift in wavelength compared to the shift caused by their initial TMV-VLP assembly (figure 7). The −3.62% resonant wavelength shift produced by the TMV*1Cys*-VLP–coated sensor suggests that the primary and secondary antibodies do not bind to the TMV1*Cys*-VLP receptor layer and may disassemble or denature some of the TMV-VLP structures in the process. The optical chip immobilized with TMV1*Cys*-VLP-*Flag*, on the other hand, shows a positive wavelength shift of 567%, resulting from the attachment of the primary Flag antibody, secondary antibody, and enzymatic substrate precipitate. The optical spectra, figure 8, show not only a shift in resonant wavelength but a decrease in optical transmission, quality factor, and signal-to-noise ratio. The significant difference between the resonant frequency shifts of the TMV1*Cys*-VLP-*Flag*– and TMV1*Cys*-VLP–coated resonators demonstrates the selectivity provided by the expressed Flag antigen on the outer surface of the TMV1*Cys*-VLP-*Flag*.

After the immobilization of TMV1*Cys*-VLP-*Flag* onto two additional microdisk resonators, primary antibody is introduced onto one sensor system and primary and secondary antibodies are sequentially introduced onto the other. Neither system underwent the enzymatic substrate reaction that typically induces the formation of colored precipitates when visual indicators are needed. It can be shown that the binding of the primary antibody and primary and secondary antibodies onto TMV-VLPs caused a shift in the resonator wavelength of 0.79 +/−0.41 nm (+51%) and 2.10 +/−0.78 nm (+135%), respectively. These increasing positive shifts correlate with an increase in effective index caused by an increase in evanescent field interaction with added cladding material. This corresponds directly to the binding of the primary antibody followed by the secondary antibody, demonstrating the ability of the sensor platform to detect the binding of analyte without labeling or visual indications. The reduced magnitude in wavelength shifts caused by antibody bindings further suggests that the 5.95 nm shift caused by the full ELISA procedures is predominantly induced by the enzymatic substrate.

An additional experiment is performed to verify the selectivity of TMV1*Cys*-VLP-*Flag* to Flag antibodies against non-fat milk. A series of microdisk resonators functionalized with TMV1*Cys*-VLP-*Flag* coatings are immersed in a non-fat milk solution, which contains a multitude of proteins, salt, and vitamins. Resonant wavelength shifts of −0.021 nm (−7.09%) and +0.124 nm (41.9%) are observed for the resonator chips immersed in non-fat milk solution and Flag antibody in non-fat milk solution, respectively. The significant difference in the wavelength shift caused by the different solutions demonstrates the ability of the sensor platform to selectively target analytes in complex biological solutions without the use of labeling. The microresonators also show negative shifts in resonant wavelength when the non-complementary antibodies, antibody His (-and antibody HA, in milk solution are introduced to the sensors.

The negative shifts in resonant wavelength are most likely due to the denaturalization or removal of bioreceptors from the surface of the optical cavity caused by the rinsing and dehydration stages. This can be seen directly by comparing the gold-coated silicon chips. The color intensity of the enzymatic substrate activity of both sets of gold-coated chips is acquired and analyzed using ImageJ software. The results, figure 9, show that the set of chips that underwent rinsing and dehydration had an overall lower color intensity compared to the chips that remained under wet condition during the entire duration of the ELISA process. The lower color intensity, across all immobilized TMV-VLP densities as shown in figure 9(b), indicates less enzymatic substrate reaction on immobilized TMV-VLP receptors.

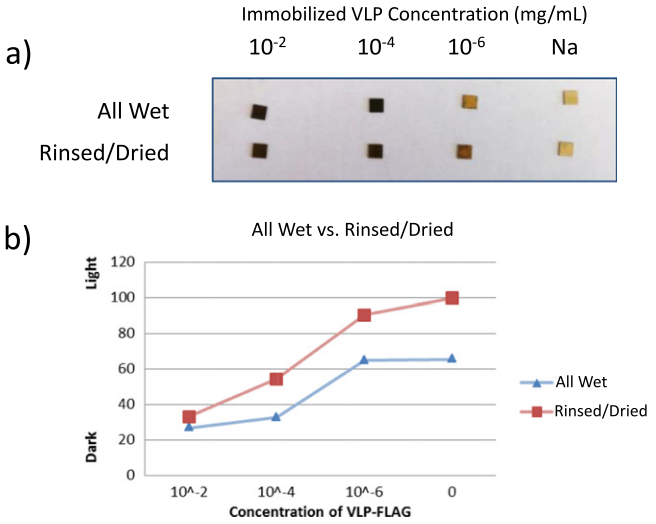

Figure 9. (a) Image showing the color intensity of ELISA conducted on gold-coated chips under all wet conditions versus rinsed and dried conditions. (b) Color intensity analysis of the two set of ELISA chips showing an overall lighter color intensity for the rinsed and dried samples.

Discussion

The microdisk resonators presented in this work are able to detect antibody binding due to the change in refractive index of their cladding, but show sporadic results when attempting to quantify the number of binding events or precise surface coverage of the nanostructures. The decrease in Q-factor from 420 to 320 and the overall optical transmission are attributed to the scattering loss induced by the attachment of nanostructures on the waveguide surfaces and in the coupling gap between the waveguide and the cavity. The amount of evanescent field interaction with the analyte binding on the surface directly influences the sensitivity of the resonator. This evanescent field interaction to a bound analyte is non-linear due to the exponential decay of the field normal to the waveguide boundary. The varying distribution of the nanostructure across the microdisk and the inevitable non-uniform distance of the bound analyte to the surface of the disk make it difficult to quantify the sensing mechanism.

The genetically conjugated TMV-VLP provides for the selectivity of the transducer, recognizing only targeted antibodies. This is made possible due to the extension of the coat protein terminal on the outer surface of the bio-nanotube. The addition of a peptide conjugation on the outer surface of the nanostructure can create a steric hindrance, which can deter the attachment of antibodies. During the development stages of the TMV-VLP synthesis, purification, and extraction, it was observed that suppression of the antigen expression on a portion of coat proteins and the insertion of a flexible linker in addition to the antigen conjugation aided in the optimization of the TMV-VLP synthesis yield. These modifications to the genetic mutation give more room for the conjugated coat protein to self-assemble into helical nanorods and provides accessibility to the flexible binding sites.

The wavelength shift induced by the TMV1*Cys*-VLP-*Flag* assembly is notably less when compared to that of TMV1*Cys*-VLP. This can be attributed to a difference between the assembly density of TMV1*Cys*-VLP and TMV1*Cys*-VLP-*Flag* on resonator sensors. The additional Flag antigen, present on the TMV1*Cys*-VLP conjugation on

the outer surface, can have unintentional effects on the properties and functionality of the TMV-VLP nanostructure. (1) The Flag-tag expression on the outer surface may disrupt the self-assembly capability of TMV-VLPs due to steric hindrance, blocking the cysteine binding site on the *n*-terminus and reducing the probability that TMV-VLPs will bind to the surface. (2) The TMV-VLPs that are bound to the substrate via the hindered cysteine may possess a weaker bond strength. As a result, during experimental stages that exert stresses on the bond, i.e. rinsing and dehydration stages, some TMV-VLPs can detach from the surface, leaving uncovered surfaces on the resonator and decreasing the sensor's effective sensitivity. (3) Flag-tag expression may also have influenced the TMV-VLP to form shorter helical rods, assembled from a smaller number of coat proteins. The immobilization of the shorter nanorods on the optical resonator results in a thinner TMV-VLP receptor layer and a reduced interaction cross-section with the evanescent wave. All these factors may contribute to the smaller wavelength shift induced by the TMV1*Cys*-VLP-*Flag* assembly compared to that of TMV1*Cys*-VLP.

Resonant wavelength shifts due to analyte attachment are quantified with respect to the resonant wavelength shift observed by their initial TMV-VLP receptor immobilization. This measurement quantification results in a relative wavelength shift percentage, rather than an absolute wavelength shift:

$$\frac{\Delta\lambda_{\text{Analyte Attachment}}}{\Delta\lambda_{\text{VLP Immobilization}}} \times 100\%.$$

This more accurately describes the binding efficiency of the receptor layer because it takes into account the number of available TMV-VLP binding sites participating in the optical interaction. An absolute measurement would be of significance only if the number of binding sites participating in the optical interrogation can be quantified and made more consistent between experiments.

The wavelength shift induced by the label-less detection of primary and secondary antibodies is also considerably smaller than the wavelength shift induced by proceeding through the entire ELISA protocol. The absence of colored solid precipitate, resulting from the substrate enzymatic reaction in the ELISA protocol, is expected to be the main cause of the effective refractive index change. The comparison between the induced shifts caused solely by the primary antibody attachment (+51%) versus the secondary antibody (+84%) is expected due the larger size of the secondary antibody.

The negative wavelength shifts observed during certain experimental stages suggests that there was a negative shift in the effective refractive index. This phenomenon was attributed to a negative index change in the cladding (receptor layer and air) rather than the waveguide itself because characterization of the silicon nitride waveguides with no assembled surface coatings showed no index changes under comparable experimental conditions. It is hypothesized that the decrease in the cladding index was due to the detachment of TMV-VLP from the resonator surface, spurred by the repeated hydration and dehydration steps in the experiment protocol. The different discoloration between the two sets of gold chip experiments, immobilized with the same TMV1*Cys*-VLP-*Flag* receptor layer, supports this claim. The darker chip set underwent the full ELISA protocol without the additional hydration and dehydration steps. The darker discoloration indicates a larger number of enzymatic reactions yielded by a larger number of Flag-tag receptors. The reduced number of Flag-tag receptors present on the lighter discolored chip is caused either by the Flag-tag receptors denaturing during this process or by the TMV-VLP's cysteine bond failing, freeing the receptor from the surface. In an earlier disk resonator experiment, a negative shift in wavelength (–0.08 nm) was observed in a control experiment that underwent dehydration and hydration of a TMV1*Cys*-VLP (without the Flag-tag)–coated chip (see figure 7).This evidence suggests that the negative shift in wavelength and the lighter discoloration of the chips are due to the detachment of TMV-VLP from the surface caused by the dehydration and hydration steps in the protocol.

The detachment of bioreceptors, which decreases the sensitivity of the system, is a limitation of the current experimental setup that requires the microtransducer to be in a dehydrated state. To circumvent the issue of repeated dehydration and hydration, measurement can be made under aqueous conditions by integrating a microfluidic system on top of the microdisk resonator. An integrated microfluidic system can further enhance the system's functionality by potentially using microchannels to assemble specific strands of TMV-VLP onto targeted resonators for multi-analyte arrayed sensing.

Conclusion

While previous work has focused on the individual sensor components presented here, this work addresses the system as a whole, including the integration of biological molecule surface assembly and microfabrication utilizing both top-down and bottom-up techniques. The development of an optical whispering gallery mode resonator, the synthesis of genetically mutated bio-nanostructures, and the successful integration of these biological receptor layers represent milestones in the field of biosensing. In particular, the results presented here demonstrate the flexibility of a TMV-VLP–based receptor layer whose genetically programmable coat protein can display a unique binding motif on transducer surfaces for specific antibodies in a wide variety of solutions. The sensitivity and selectivity of the sensor platform enable label-free detection, creating new sensing opportunities where labeling is impractical or impossible. We believe that this work provides an attractive solution to challenges present in conventional systems that utilize a wide range of polymers or metals for nonspecific bindings by utilizing the very specific nature of biological antibody-binding interactions while simultaneously increasing the variety of target analytes due to the programmability of these coatings.

Acknowledgments

This work was supported by the NSF Nanomanufacturing Program (NSF-CMMI 0927693) and the Biochemistry Program of the Army Research Office (W911NF1110138). The authors would also like to acknowledge the staff at the Maryland Nanocenter clean-room facilities and Nanoscale Imaging Spectroscopy and Properties Lab.

References

[1] Ben-Yoav H, Dykstra P H, Bentley W E and Ghodssi R 2014 A controlled microfluidic electrochemical lab-on-a-chip for label-free diffusion-restricted DNA hybridization analysis *Biosensors Bioelectron.* **64** 579–85

[2] Suleiman A A and Guilbault G G 1994 Recent developments in piezoelectric immunosensors. A review *Analyst* **119** 2279–82

[3] Jaworski J W, Roarane D, Huh J H, Majundar A and Lee S W 2008 Evolutionary screening of biomimetic coatings for selective dectection of explosives *Langmuir* **24** 4938–43

[4] Petrenko V A and Vodyanoy V J 2003 Phage display for detection of biological threat agents *J. Microbiol. Methods* **53** 253–62

[5] Gerasopoulos K, McCarthy M, Banerjee P, Fan X, Culver J N and Ghodssi R 2010 Biofabrication methods for the patterned assembly and synthesis of viral nanotemplates *Nanotechnology* **21** 1–11

[6] Fan X Z, Naves L, Siwak N P, Brown A D, Culver J N and Ghodssi R 2013 A Novel Virus-like-particle (VLP) bioreceptor coated optical disk resonator for biosensing *2013 MRS Spring Meeting (San Francisco, CA, April 1–5)*

[7] Fan X Z, Siwak N P, Brown A D, Culver J N and Ghodssi R 2012 Integration of functionalized biological nanostructures with conventional transducer fabrication schemes *American Vacuum Society 59th Int. Symp. (Tampa, FL, 28 October–2 November)*

[8] Royston E S, Brown A D, Harris M T and Culver J N 2009 Preparation of silica stabilized Tobacco mosaic virus templates for the production of metal and layered nanoparticles *J. Colloid Interface Sci.* **332** 402–7

[9] Fan X Z, Pomerantseva E, Gnerlich M, Brown A, Gerasopoulos K, McCarthy M, Culver J and Ghodssi R 2013 *Tobacco mosaic virus*: a biological building block for micro/nano systems *J. Vac. Sci. Technol.* A **31** 050815–1 *Invited*

[10] Matsko A B, Savchenkov A A, Strekalov D, Ilchenko V S and Maleki L 2005 Review of applications of whispering-gallery mode resonators in photonics and nonlinear optics *IPN Progress Report* vol 42 available at http://mechatronics.poly.edu/Control_Lab/Padmini/WGMLitSurvey/WGMReview.pdf

[11] Rayleigh L 1912 The problem of the whispering gallery *Phil. Mag.* **20** 1001–4

[12] Zhu H, White I M, Suter J D, Zourob M and Fan X 2008 Opto-fluidic micro-ring resonator for senstivie label-free viral detection *Analyst* **133** 356–60 2007

[13] Fan X, White I M, Zhu H, Suter J D and Oveys H 2007 Overview of novel integrated optical ring resonator bio/chemical sensors *Proc. SPIE* **6452** 1–20

[14] Brown A, Naves L, Wang X, Ghodssi R and Culver J N 2013 Carboxylate directed *in vivo* assembly of virus-like nanorods and tubes for the display of functional peptides and residues *Biomacromolecules* **14** 3123–9

[15] Cho J-H, Han S-M, Paek E-H, Cho I-H and Paek S-H 2006 Plastic ELISA-on-a-chip based on sequential cross-flow chromatography *Anal. Chem.* **78** 793–800

[16] Jeon J-W, Seo S-M, Kim H-S, Oh J-S, Oh Y-K, Ha G-W, Hwang S-Y and Paek S-H 2012 ELISA-on-a-chip for on-site, rapid determination of anti-rabies virus antibodies in canine serum *Sensors Actuators* B **171–172** 278–86

[17] Rasooly A, Bruck H and Kostov Y 2013 An ELISA Lab-on-a-Chip (ELISA-LOC) *Microfluidic Diagnostics* vol 949 ed G Jenkins and C D Mansfield (New York: Humana Press) pp 451–71

[18] Gerasopoulos K, McCarthy M, Royston E, Culver J N and Ghodssi R 2008 Nanostructured nickel electrodes using the *Tobacco mosaic virus* for microbattery applications *J. Micromech. Microeng. (JMM)* **18** 1–8

[19] Gnerlich M, Pomerantseva E, Gregorczyk K, Ketchum D, Rubloff G and Ghodssi R 2013 Solid flexible electrochemical supercapacitor using Tobacco mosaic virus nanostructures and ALD ruthenium oxide *J. Micromech. Microeng.* **23** 114014